Link-Level Abstraction of IEEE 802.11ay based on Quasi-Deterministic Channel Model from Measurements

Neeraj Varshney, Jiayi Zhang, Jian Wang, Anuraag Bodi, and Nada Golmie
Wireless Networks Division, National Institute of Standards and Technology, Gaithersburg, MD 20899 USA
Emails: {neeraj.varshney, jiayi.zhang, jian.wang, anuraag.bodi, nada.golmie}@nist.gov

***Abstract*—In this paper, we analyze the performance of link-level abstraction for orthogonal frequency-division multiplexing (OFDM) and single-carrier (SC) modes in IEEE 802.11ay wireless systems over the 60 GHz millimeter-wave band. In particular, we evaluate the effectiveness of the three existing effective signal-to-noise ratio (SNR) metric (ESM) schemes (i.e., exponential ESM (EESM), mean mutual information per coded bit (MMIB) and post-processing ESM (PPESM)). Furthermore, to deal with the issue that EESM calibration is dominated by channel realizations with poor error performance, we introduce a classification based EESM (CEESM) scheme with a new metric named coefficient of variation, which is used to measure the severity of frequency-selective fading. Finally, we present several important insights developed through extensive experimentation. Based on our validation results, the MMIB and PPESM can be employed with minimum computational complexity for OFDM and SC modes, respectively. In contrast, EESM and CEESM can be considered for both modes with better accuracy, but at a cost of high implementation complexity.**

***Index Terms*—Link-level abstraction, IEEE 802.11ay, Quasi-Deterministic channel model, Millimeter-wave**

I. Introduction

IEEE 802.11ay is an enhanced wireless local access network (WLAN) standard that is capable of achieving high throughput and high power efficiency based on its predecessor, IEEE 802.11ad standard [1]. In IEEE 802.11ay, the wireless transceiver operates in the 60 GHz millimeter-wave (mmWave) band with the aid of directional antenna beams. During the development of the 802.11ay standards, several algorithms and solutions have been proposed to improve system performance. Thus, how to evaluate the system performance with high fidelity is critical. Particularly, the physical (PHY) layer is an essential component in wireless systems and its performance directly affects the overall system performance.

For an instantaneous channel realization, it is important to predict the link-level performance, such as packet error rate (PER) or packet success rate (PSR), for different PHY-layer configurations (e.g., modulation and coding schemes (MCS), and antenna configurations) so that whether a packet was transmitted successfully or not can be determined. As it is not feasible to run the time-consuming symbol-by-symbol link-level simulation (LLS) simultaneously with the system-level simulation (SLS), a PHY-layer abstraction model should be used to predict the decoding results based on the multi-path properties of fading channels. This motivates us to focus on assessing the effectiveness of methods that can be used to abstract the PHY-layer performance of IEEE 802.11ay over the 60 GHz mmWave channel.

Existing research efforts have been conducted on link-to-system (L2S) level mapping [2]–[8]. Most of these works [2]–[5] have focused on the orthogonal frequency-division multiplexing (OFDM) systems, while a few other works [6], [7] have emphasized single-carrier (SC) systems for the Long-Term Evolution (LTE) uplink, which are all operated in the sub-6 GHz spectrum. Recall that IEEE 802.11ay WLAN operates in the 60 GHz mmWave band, which has unique characteristics in comparison to sub-6 GHz channels, including sparse signal paths raised by higher penetration loss, weaker diffraction, and higher directional signals introduced by the beamforming technology [9], among others. Thus, in this paper, we address the following issues: *(i) whether existing L2S mapping approaches are still suitable for mmWave OFDM communications, (ii) whether existing L2S mapping approaches can be applied to IEEE 802.11ay SC mode as they have been used in orthogonal frequency-division multiple access (OFDMA) and SC-FDMA systems, and (iii) unlike previous work using PER, we consider bit error rate (BER), which offers flexibility in media access control (MAC) layer to derive PER if packets are partially overlapped in time domain or frequency domain.* To address the aforementioned issues, in this paper we investigate and compare different L2S abstraction schemes for IEEE 802.11ay single-input single-output (SISO) communication for both SC and OFDM modes as an initial step of our project. Once we gain enough confidence in single-link abstraction schemes, we will extend our work for multiple-input and multiple-output (MIMO) systems.

In this paper, our primary contributions are as follows: (i) *We develop a LLS by incorporating the Quasi-Deterministic (Q-D) model extracted from mobile empirical measurements.* We conduct an IEEE 802.11ay LLS for both SC and OFDM modes based on the Q-D channel model, which emulates a lecture room (LR) environment. (ii) *Based on LLS results, we evaluate the effectiveness of the three existing effective signal-to-noise ratio (SNR) metric (ESM) schemes*, i.e., exponential ESM (EESM) [5], mean mutual information per coded bit (MMIB) [2] and post-processing ESM (PPESM) [7]. For EESM, the LLS results are used to calibrate the parameters, which are used to map subband signal-to-noise ratios (SNRs) to the effective SNR. For MMIB and PPESM, the LLS is used to validate the effectiveness of the SNR mapping, since no calibration is required. Further, to deal with the issue that EESM calibration is dominated by channel realizations with poor BER performance, we introduce a classification based EESM (CEESM) scheme with a new metric named coefficient of variation (CV), which is used to measure the severity of the frequency-selective fading. With CEESM, the prediction accuracy of the BER performance for an instantaneous channel realization can be improved. Further note that, to the best of our knowledge, this is the first work which evaluates the ESM schemes on 802.11ay systems based on Q-D channel model. (iii) *We conduct extensive experiments in three environments to validate the effectiveness of the aforementioned schemes.*

The remainder of the paper is organized as follows. In Section II, we introduce the system model and preliminaries including the Q-D channel model, LLS and subband SNRs. In Section III, we present several L2S mapping schemes for OFDM and SC modes in detail. In Section IV, we present the simulation results. Finally, we conclude the paper in Section V.

II. System Model and Preliminaries

A. Q-D Channel Model

To model the channel, the two communication devices (i.e., transmitter (TX) and receiver (RX)) are randomly deployed in a LR of size 10 m × 19 m × 3 m. The phased-array-antenna with 5-by-5 antenna elements is used at both TX and RX. In our setup, we assume that the beam selection phase has been completed, and the optimum beam direction has been selected to achieve the maximum receive power. With a TX and RX pair, we use the Q-D channel realization software developed by the National Institute of Standards and Technology (NIST) to realize the channel [9]. The Q-D channel realization software has two major engines, a deterministic engine and a stochastic engine, to compute the rays between TX and RX. The deterministic engine generates deterministic rays, also referred to as specular rays using the ray-tracing method. On the other hand, the stochastic engine regenerates diffused rays, which are clustered around the specular rays using the Q-D parameters extracted from NIST measurement campaign [10]. In our realization, we only consider reflections up to 2nd order and each of the rays is characterized by the path gain, the delay τ, the angle-of-arrival (AOA) θ^R at the RX, and the angle-of-departure (AOD) θ^T from the TX. The generated Q-D rays are then analog beamformed by the TX and RX antenna arrays to generate the multipath between TX and RX. The detailed description about the Q-D channel model can be found in [9]. Based on this model, the impulse response of the beamformed channel is given as,

$$h(t) = \sum_{\tau}\sum_{\theta^T}\sum_{\theta^R} G^T(\theta^T)G^R(\theta^R)h(t,\tau,\theta^T,\theta^R), \quad (1)$$

where $G^T(\theta^T)$ and $G^R(\theta^R)$ represent the transmit and receive antenna beam patterns that weight each ray based on its direction. By combining all the rays falling into a sampling interval T_s, the channel is converted to a tap-delay profile, where the Kth tap is given as,

$$h(t,K) = \sum_{\tau=(K-1)T_s}^{KT_s}\sum_{\theta^T}\sum_{\theta^R} G^T(\theta^T)G^R(\theta^R)h(t,\tau,\theta^T,\theta^R). \quad (2)$$

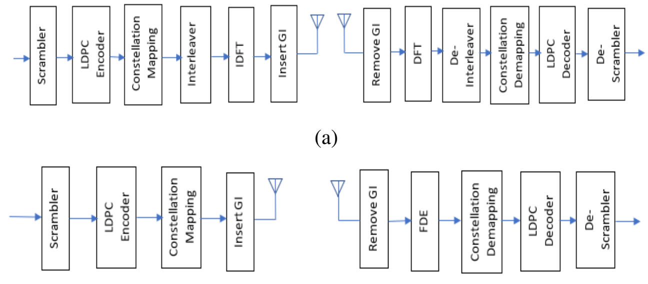

Fig. 1: Transceiver diagrams of (a) OFDM mode and (b) SC mode

The channel impulse response $h(t,k) = \sum_K h(t,K)\delta(k-K)$ at the time t is subsequently used in LLS to obtain the fading channel performance. Note that t denotes the packet realization time in our simulation, and a new channel realization is generated for every packet to be transmitted.

B. Link-level Simulation (LLS)

The transceiver diagrams of the OFDM and SC modes are shown in Fig. 1(a) and Fig. 1(b), respectively. In this work, we assume that the perfect channel knowledge is available at the RX. Also, the PHY-layer impairments (carrier frequency offset, phase noise, etc.) are not included in the LLS. In the evaluation, the symbol-by-symbol simulation is performed. The packet size is considered as 4 096 bytes for both SC and OFDM modes. Note that in our simulation, the performance metric is the BER, which can be employed to compute the PER based on the transmit PSDU packet size. The end-to-end simulation is based on the 802.11ad implementation in the MATLAB WLAN Toolbox[1] with the extension to include 802.11ay specific MCSs. Moreover, we assume that the fading channel is semi-static and does not change within a packet transmission duration.

With the LLS, we obtain the BER performance as a function of SNR over additive white Gaussian noise (AWGN) channel and multi-path fading channels derived from the Q-D channel model for various MCSs. The AWGN performance can be stored in a network simulator such as ns3 so that BER can be directly retrieved based on mapped effective SNR. In the meantime, these decoding results obtained using the Q-D channel model for the LR environment, along with its instantaneous channel tap-delay profiles and the AWGN performance curve, will be used to calibrate the mapping parameters in EESM.

In addition, we use these fading channel decoding results to validate the effectiveness of SNR mapping by measuring the difference between the SNR of the AWGN channel and the mapped effective SNR given a channel realization for the same BER value. Note that the L2S mapping is to find the AWGN equivalent SNR (effective SNR) of the channel, and use the effective SNR to obtain the channel decoding performance (i.e., BER or PER) from the stored AWGN link performance

[1] Certain commercial equipment, instruments, or materials are identified in this paper in order to specify the experimental procedure adequately. Such identification is not intended to imply recommendation or endorsement by the NIST, nor is it intended to imply that the materials or equipment identified are necessarily the best available for the purpose.

curves. Also, note that the calibration and validation are MCS and PHY mode dependent. The SC mode supports MCS 1 to MCS 21, and the modulation schemes are $\pi/2$-binary phase shift keying (BPSK), $\pi/2$-quadrature PSK (QPSK), $\pi/2$-16-quadrature amplitude modulation (QAM), and $\pi/2$-64-QAM for MCS 1 to MCS 6, MCS 7 to MCS 11, MCS 12 to MCS 16, and MCS 17 to MCS 21, respectively. Moreover, the OFDM mode supports BPSK, QPSK, 16-QAM, 64-QAM for MCS indices 1 to 5, 6 to 10, 11 to 15, and 16 to 20, respectively.

C. Subband SNRs

The subband SNRs are used to compute the effective SNR of a wide-band channel[2]. For this purpose, we first need to compute the center frequency of each subband and then derive the received subband SNRs in OFDM and SC Modes.

For a given wide-band channel of bandwidth B and its center frequency f_c, the center frequency of the nth subband can be obtained as, $f_{c,n} = f_c + n\Delta f$, where the subband spacing Δf considering the number of N_{ST} subbands is computed as, $\Delta f = \frac{B}{N_{\text{ST}}}$. Here $n = -\text{round}\left(\frac{N_{\text{ST}}}{2}\right) + 1, \cdots, \text{floor}\left(\frac{N_{\text{ST}}}{2}\right)$, where floor$(x)$ rounds the elements of x to the nearest integers towards $-\infty$ and round(x) rounds towards the nearest decimal or integer. In OFDM mode, each subband corresponds to a subcarrier with subcarrier spacing $\Delta f = 5.156\,25\,\text{MHz}$; while for SC mode, the entire bandwidth B is divided into $N_{\text{ST}} = 512$ subbands with $f_{c,n} = f_c + (n - \frac{1}{2})\Delta f, n = -(\frac{N_{\text{ST}}}{2} - 1), \cdots, \frac{N_{\text{ST}}}{2}$ to match the 512-point frequency-domain equalizer (FDE) adopted at the RX. The frequency-domain channel transfer function (CTF), which is defined as the Fourier transform of the impulse response $h(t)$ at subband center frequency $f_{c,n}$, can be obtained as, $H_{\text{BF}}(f_{c,n}) = \sum_{l=0}^{L-1} h(t,l)\exp(-j2\pi f_{c,n} l T_s)$, where T_s is the sampling period, l is the tap index, and L is the number of sampled multi-path. The received SNR for nth subband corresponding to the transmission over a SISO beamformed channel with power P can be derived by,

$$\gamma_n = \frac{P|H_{\text{BF}}(f_{c,n})|^2}{N_0}. \tag{3}$$

Here, the AWGN power N_0 is BkT for SC mode, where $k = 1.3807 \times 10^{-23}$ J/K is Boltzman constant, $T = 290$ is ambient temperature in degree Kelvin, and the bandwidth is $B = 2.16\,\text{GHz}$. For OFDM mode, $N_0 = NB_{\text{SB}}kT$, where the subcarrier bandwidth $B_{\text{SB}} = 5.156\,25\,\text{MHz}$ and $N = N_{\text{SD}} + N_{\text{SP}}$ denotes the total number of data and pilot subcarriers (i.e., $N = 336 + 16 = 352$) for a single $2.16\,\text{GHz}$ channel.

III. Link-to-System (L2S) Mapping Schemes

In order to evaluate the system wide performance for a wireless network with numerous transmission links and interference among multiple wireless nodes, the SLS requires the link-level performance in terms of the channel condition (e.g., signal-to-noise ratio and channel state information subject to multi-path fading) and system parameters, which provides the prediction of the instantaneous transmission qualities over specific individual links. L2S can provide such prediction without running through PHY-layer symbol-by-symbol simulation which can introduce very large simulation overhead.

[2]Note that a single contiguous $2.16\,\text{GHz}$ channel with $f_c = 60.48\,\text{GHz}$ is considered in this study.

Generally speaking, the L2S mapping is a class of methods to perform the PHY-layer abstraction and provide the prediction of error performance at a SNR in system-level. In the following sub-sections, we first introduce the effective SNR metric for the L2S mapping and subsequently present the EESM, MMIB, PPESM and CEESM schemes in detail.

A. Effective SNR Metric (ESM)

ESM provides the PHY-abstraction metric for L2S mapping which is an interface between the LLS and SLS [11]. Due to multi-path, the channel experiences frequency selective fading, meaning that channel frequency response is no longer flat and each frequency subband may have different gain. According to [12], for a given subband SNR vector of size N corresponding to a fading channel, the scalar effective SNR is defined as an equivalent SNR over AWGN channel, which would yield the same frame/ packet error probability. Note that the error performance curves over AWGN channel are MCS and PHY mode (i.e. SC or OFDM) dependent. For a given PHY mode and MCS, the mapping of the error performance between a specific fading channel and AWGN channel is represented by the AWGN equivalent SNR provided by EESM, MMIB, and PPESM. Based on the mapping function, the SLS can directly use the AWGN lookup tables to find the BER or PER corresponding to the data transmission through the multi-path fading channel.

Using a general L2S mapping technique with mapping function $\Phi(\cdot)$, the effective SNR γ_{eff} can be calculated as,

$$\gamma_{\text{eff}} = -\beta_1 \Phi^{-1}\left(\frac{1}{N}\sum_{n=1}^{N}\Phi\left(-\frac{\gamma_n}{\beta_2}\right)\right), \tag{4}$$

where $\Phi^{-1}(\cdot)$ is the inverse mapping function of $\Phi(\cdot)$, and β_1 and β_2 are the scalar parameters which need to be optimized for different MCSs.

B. EESM

The EESM replaces the function $\Phi(\cdot)$ with the exponent function assuming that all the subcarriers are modulated using the same MCS. The mapping of EESM is given as,

$$\gamma_{\text{eff}} = -\beta \ln\left(\frac{1}{N}\sum_{n=1}^{N}\exp\left(-\frac{\gamma_n}{\beta}\right)\right), \tag{5}$$

where $\beta_1 = \beta_2 = \beta$ and $N = N_{SD}$ for OFDM mode. Similarly, we extend the EESM for SC mode with $N = N_{\text{ST}}$ subbands. In contrast to $N_{\text{SD}} = 336$ data subcarriers in OFDM mode, the above expression for SC mode considers all the $N_{\text{ST}} = 512$ subbands as the transmitted SC signal covers the entire bandwidth of $2.16\,\text{GHz}$. The tuning parameters β_{OFDM} and β_{SC} in Table I for 802.11ay OFDM and SC modes are calibrated based on the AWGN curves and the aggregated Q-D fading channel results with 600 random channel realizations and 161 SNR points for each realization. Note that this work

MCS Index	Optimal β_{OFDM}	MSE (dB)
1	1.60	-15.68
2	1.34	-14.43
3	1.29	-13.46
4	1.42	-12.67
5	1.25	-10.96
6	1.47	-11.07
7	1.75	-9.665
8	1.63	-8.477
9	1.82	-7.077
10	1.81	-6.038
11	3.89	-3.536
12	4.93	-1.884
13	5.37	-0.348
14	5.64	1.804
15	6.53	2.543
16	13.81	6.876
17	13.11	8.819
18	24.43	10.73
19	25.94	12.18
20	31.02	14.35

MCS Index	Optimal β_{SC}	MSE (dB)
1	0.21	-46.98
2	0.58	-42.44
3	0.87	-33.37
4	1.07	-33.18
5	1.31	-28.86
6	1.47	-26.38
7	1.15	-25.52
8	1.49	-23.27
9	1.82	-18.86
10	2.04	-16.98
11	2.24	-13.76
12	1.90	-9.030
13	2.92	-4.449
14	3.96	-0.241
15	4.71	1.781
16	6.68	4.352
17	4.49	1.290
18	7.37	6.094
19	11.51	10.97
20	14.33	13.65
21	20.50	16.27

TABLE I: Optimal β_{OFDM} and β_{SC} for OFDM and SC modes, respectively, which minimizes the mean-squared error (MSE) between AWGN SNR and predicted SNR vectors for same BER values.

combines all the channel realizations considered in CEESM while optimizing the tuning parameter in EESM.

C. MMIB based ESM

The MMIB based ESM was introduced for OFDM mode in IEEE 802.16m [2] and it was recently recommended in the evaluation methodology of IEEE 802.11ay standardization [13]. In MMIB, the function $\Phi(\cdot)$ maps each bit-channel to a mutual-information (MI) value, i.e., the capacity of the bit-channel [2]. The MMIB of the wide-band channel $\overline{I}_m$ is then computed by averaging the MIs of all bit-channels as, $\overline{I}_m = \frac{1}{N}\sum_{n=1}^{N} I_m(\gamma_n)$, where $N = N_{SD}$ for OFDM, $N = N_{ST}$ for SC, and m is the modulation order with value $m = \{1, 2, 4, 6\}$ representing BPSK, QPSK, 16-QAM, and 64-QAM, respectively. The term $I_m(\gamma_n)$ computes the MI per bit for nth subband with modulation order m as a function of nth subband SNR γ_n. Then, the reverse mapping function $I_m^{-1}(\overline{I}_m)$ is used to map the MI of the wide-band channel back to its effective SNR as described in [2, Section 3.2.1.5]. Since it is difficult to obtain the inverse function in a closed-form during implementation, especially for higher order modulations, we use a table-lookup method[3] to obtain the effective SNR from averaged MI.

D. Post-Processing ESM (PPESM) for SC-FDE

When communicating over a frequency-selective fading channel, both OFDM and SC modes employ FDE using various algorithms, i.e., matched-filtering (MF), zero-forcing (ZF), or the minimum MSE (MMSE), for post-processing at the RX. Further note that the channel encoding/decoding and symbol modulation/demodulation in OFDM mode are processed in frequency-domain directly; while these processes in SC mode are performed in time-domain. Thus, the OFDM modulated symbol can be recovered directly after one-tap equalization. However, in SC mode, the modulated symbols within a time-domain transmit block interfere with each other, which results in a residual interference among modulated symbols within a SC block after FDE operation, namely the inter-symbol-interference (ISI)[4]. Note that the residual ISI limits the system performance unless interference cancellation or decision-feedback equalization is introduced [14].

Considering the perfect CSI at the RX, the post-processing SNR of SC-FDE can be expressed as [7], $\gamma_{\text{SC}} = \frac{\mathcal{S}}{\mathcal{I}+\mathcal{N}}$, where the post-processing received signal power $\mathcal{S} = P\left|\frac{1}{N_{\text{ST}}}\sum_{n=1}^{N_{\text{ST}}} W_n^* H_n\right|^2$, the post-processing noise power $\mathcal{N} = \frac{N_0}{N_{\text{ST}}}\sum_{n=1}^{N_{ST}} |W_n|^2$, and the post-processing residual ISI power $\mathcal{I} = P\Big(\frac{1}{N_{\text{ST}}}\sum_{n=1}^{N_{\text{ST}}} |W_n^* H_n|^2 - \left|\frac{1}{N_{\text{ST}}}\sum_{n=1}^{N_{\text{ST}}} W_n^* H_n\right|^2\Big)$. Note that H_n and W_n represent the frequency-domain channel gain and corresponding FDE weight at the nth subband, respectively. Since the SC mode in our study employs a classic linear MMSE-FDE, its post-processing SNR can be derived as,

$$\gamma_{\text{SC}}=\left[\left(\frac{1}{N}\sum_{n=1}^{N}\frac{\gamma_n}{\gamma_n+1}\right)^{-1}-1\right]^{-1}=\left(\frac{1}{N_{\text{ST}}}\sum_{n=1}^{N_{\text{ST}}}\frac{1}{\gamma_n+1}\right)^{-1}-1, \quad (6)$$

where γ_n is given by Eq. (3). Consequently, the Eq. (6) can be expressed as the effective SNR γ_{eff} in Eq. (4), having a function of $\Phi(\gamma_n) = (\gamma_n + 1)^{-1}$. We refer to this scheme as PPESM for SC-FDE.

E. Channel Classification Based EESM

1) Classification of Channel Realizations: For 60 GHz mmWave-channel model, the performance of the system varies significantly between different TX and RX locations. Apart from this, different realizations for fixed locations of TX and RX also affect the performance drastically. If we use all the channel realizations while optimizing the parameters for mapping schemes (e.g. EESM), the system performance is always dominated by the worse channel realizations. Thus, the parameters optimized for various mapping schemes cannot be considered for realizations that experience frequency-flat fading.

To address this issue, we propose the channel classification based mapping scheme, in which channel realizations are grouped in different segments before obtaining the optimal parameters for mapping schemes. It is important to note that the random channel realizations can be easily divided into different segments using the metric such as 'CV'. The CV value using the N subcarrier channel gains, i.e., $|H_{\text{BF}}(f_{c,n})|, 1 \leq n \leq N$, for a given channel realization is computed as[5],

$$CV = \frac{std(|H_{\text{BF}}(f_{c,n})|, n = 1, 2, \cdots, N)}{mean(|H_{\text{BF}}(f_{c,n})|, n = 1, 2, \cdots, N)}, \quad (7)$$

[3]To apply the inverse function, we read the lookup table, and locate the closest SNR value for an input value of MI.

[4]The MF and MMSE based FDEs introduce the residual ISI. The ZF FDE completely eliminate the residual ISI, but the noise may be amplified when a deep frequency-domain fade is encountered.

[5]It is important to note that we consider subcarrier channel gains in CV to avoid the dependency on the transmit power while characterizing the channel realizations into different segments.

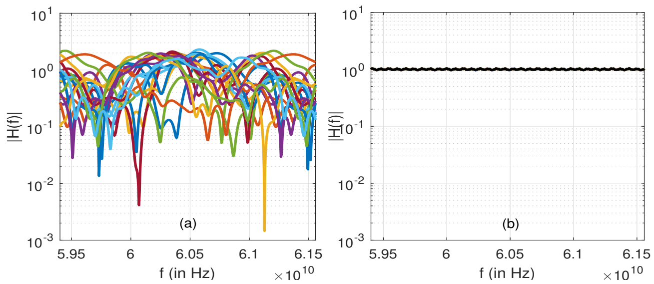

Fig. 2: CTF of randomly generated channel realizations for (a) segment 1 when CV > -2 dB, and (b) segment 6 when CV < -6 dB

where $std(\cdot)$ and $mean(\cdot)$ denote the standard deviation and mean, respectively. For a channel realization with high frequency-selective fading, the CV value would be very high in comparison to the frequency-flat fading channel. This can be clearly seen in Fig. 2, in which the channel realizations are divided into six segments using five thresholds with 1 dB spacing, i.e., $(-2, -3, -4, -5, -6)$ dB. From Fig. 2(a), we can observe that the segment 1 consists of all the channel realizations with $CV > -1$ dB and suffer from very high frequency-selective fading. In contrast to this, each realization in segment 6 with $CV < -6$ dB experiences almost frequency-flat fading, which can be clearly seen in Fig. 2(b).

2) Applying Classification to EESM: Using K thresholds, we first divide the channel realizations into $K+1$ segments and then calibrate the EESM parameter (β) using the channel realizations belonging to a particular segment only. By doing this, the prediction error can be significantly reduced, particularly when the channel experiences frequency-flat fading.

In order to map subband SNRs to the effective SNR of the channel, we first categorize the channel to a segment[6] based on the CV value as shown in Fig. 3. We then use the segment and MCS specific mapping function (i.e. specific β value) to perform the effective SNR mapping in EESM. The EESM parameters[7] corresponding to six segments for OFDM and SC modes are presented in Table II, respectively. It can be observed in Tables I and II that the optimal β values for EESM are approximately identical to the ones obtained for segment 1 in CEESM. This is owing to the fact that the system performance is always dominated by the worse channel realizations in EESM. Further, it is worth noting that the optimal β values for segment 6 are different than segment 1.

IV. Performance Evaluation

This section presents simulation results to validate the performance of various mapping methods over 60 GHz mmWave

[6]This work divide all the channel realizations into six segments using five thresholds and compute six EESM parameters for each MCS.

[7]To obtain these parameters, we considered 100 random channel realizations in each segment and simulated 161 SNR points for each random channel realization, having receive power ranging from -120 dBm to -80 dBm with a spacing of 0.25 dBm and a MCS dependent SNR offset. In SC mode, we consider SNR offsets of $(0, 5, 10, 15)$ dBm for MCS indices 1 to 6, 7 to 11, 12 to 16, and 17 to 21, respectively. In OFDM mode, we consider SNR offsets of $(0, 5, 10, 15)$ dBm for MCS indices 1 to 5, 6 to 10, 11 to 15, and 16 to 20, respectively.

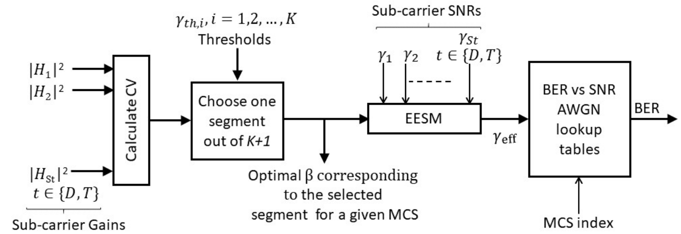

Fig. 3: Schematic Block Diagram for CEESM

TGay channel model [15] developed by the NIST and MATLAB. We configure the MATLAB TGay channel model to have an access point (AP) with a 2-by-2 TX antenna array at a height of 6 m in an open area hotspot (OAH) environment, and an AP TX at 6 m in height with a 4-by-4 antenna array for a large hotel lobby (LHL) environment. In both OAH and LHL environments, the station (STA) has a RX height of 1.5 m. Since the antenna array sizes are not specified in [15], we configure the OAH and LHL environments using different antenna array sizes in order to simulate diverse beam patterns.

For simulation purposes, various system parameters are considered as follows. For both SC and OFDM modes, long guard interval length, i.e., 192 for OFDM and 128 for SC, is considered to reduce the interference between concatenated SC or OFDM transmission blocks[8], namely inter-block interference (IBI), especially for the scenario where the channel experiences large path delay. The PSDU packet length is set as 4 096 bytes, i.e, the number of bits transmitted within a packet (L_{bits}) is 32 768. It is worth noting that to implement the L2S mapping in SLS, the PER (P_{pe}) can be easily obtained from BER (P_{be}) as $P_{pe} = 1-(1-P_{be})^{L_{\text{bits}}}$ for any arbitrary packet size. Thus, in contrast to using PER-based lookup tables, the BER-based lookup tables can be used for any arbitrary packet size to decide its PSR. All the mapping schemes are validated over a total of 1 000 random channel realizations. For each packet transmission, the transmit signal power is randomly selected so that the receive signal power is among a range with a step size[9], plus a MCS-dependent offset[6].

From Fig. 4, it can be clearly seen that the predicted BER values obtained using the optimal β_k (c.f. Table II) in CEESM effective SNR match well with the actual BER for low as well as high MCSs in both OFDM and SC modes. It can also be observed in Fig. 4 that the optimal mapping parameters obtained through the NIST LR environment are also applicable to various MATLAB TGay-channel environments, including LHL and OAH. Using EESM and CEESM, the MSE between the AWGN SNR and predicted SNR vectors for the same BER values under various environments are given in Table III. It can be clearly seen that the CEESM performs well in comparison to the EESM.

Comparing to EESM and CEESM, MMIB and PPESM

[8]We describe an OFDM symbol as an OFDM block in order to apply the same term to both OFDM and SC modes.

[9]The receive signal power range is given by: (i) EESM/CEESM: -120 dBm to -95 dBm with a step size of 0.5 dBm, and (ii) MMIB/PPESM: -120 dBm to -90 dBm with a step size of 0.05 dBm.

Mode	MCS Index	β_1	MSE	β_2	MSE	β_3	MSE	β_4	MSE	β_5	MSE	β_6	MSE
OFDM	1	1.63	-15.68	1.38	-16.77	1.68	-17.69	1.54	-17.69	2.09	-17.69	3.97	-18.86
	6	1.40	-10.86	1.35	-12.84	1.44	-13.01	1.81	-13.27	1.62	-14.09	4.98	-16.77
	11	4.78	-2.716	4.25	-3.269	3.92	-4.948	4.37	-5.436	3.26	-6.882	1.29	-10.75
	16	13.3	7.740	14.3	6.194	16.5	5.109	14.4	3.386	13.5	3.244	9.63	0.633
SC	2	0.83	-34.94	0.73	-35.85	0.72	-32.29	0.58	-30.22	0.51	-28.86	0.12	-34.55
	7	1.23	-23.09	1.24	-24.81	1.25	-24.20	1.24	-24.43	1.16	-24.09	0.49	-27.69
	12	2.51	-3.565	2.56	-5.482	2.21	-7.772	2.34	-8.601	2.31	-10.60	0.87	-19.58
	17	4.50	4.242	4.55	2.624	4.65	1.903	5.55	0.277	5.62	-3.251	5.37	-8.794

TABLE II: Optimal $\beta_{\mathrm{OFDM},k}, \beta_{\mathrm{SC},k} = \beta_k, 1 \leq k \leq 6$ corresponding to six segments for 802.11ay OFDM and SC modes

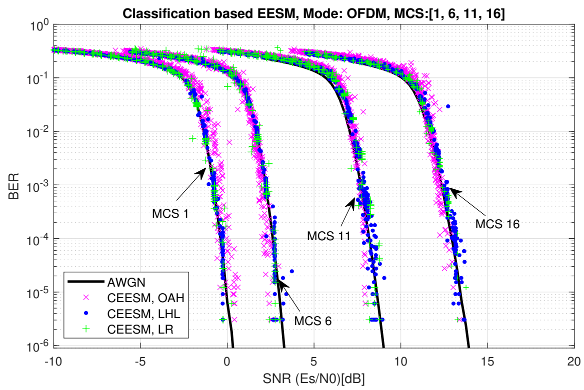

(a) 802.11ay (EDMG-PHY) OFDM mode

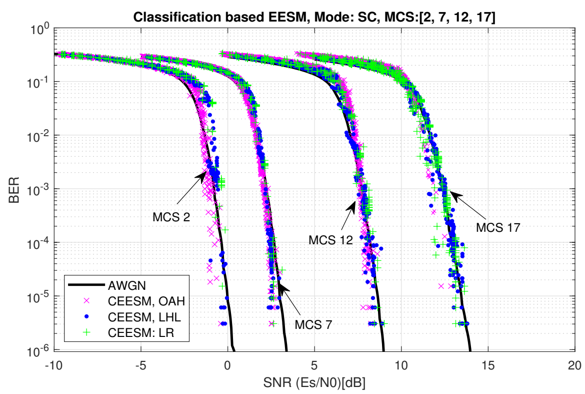

(b) 802.11ay (EDMG-PHY) SC mode

Fig. 4: Classification based EESM validation considering various MCSs (BPSK, QPSK, 16-QAM, 64-QAM all in $1/2$ code rate) with various 60 GHz mmWave multi-path fading channel models

are generic and do not require any calibration. Figs. 5(a) and 5(b) show the BER/SNR validation results of MMIB scheme for OFDM and SC modes in various mmWave channel environments, i. e. NIST TGay LR, Matlab TGay LHL, and OAH. In Fig. 5(a), the predicted BER samples of OFDM mode using MMIB over channel realizations of all three environments closely match to the BER obtained through LLS over AWGN channel. As we observe that a few outliers exist for higher MCSs, the OFDM packet transmission over Matlab TGay LHL channel occasionally result in a high error rate despite of high SNR, as shown in Fig. 5(a). These few outliers in turn results in the high MSE values in Table IV[10]. The

[10]The MSE values 18.89 dB and 26.53 dB for MMIB OFDM MCS 11 and MCS 16 are obtained when the IBI is considered with the presence of corresponding channel realizations. Otherwise, the MSE values -6.19 dB and 1.02 dB are calculated with the absence of these realizations causing IBI.

MCS Index	CEESM OFDM LR	CEESM OFDM OAH	CEESM OFDM LH	EESM OFDM LR	EESM OFDM OAH	EESM OFDM LHLL
1	-31.35	-24.82	-32.12	-29.16	-23.05	-30.31
6	-24.01	-22.18	-25.95	-22.79	-21.99	-24.90
11	-6.97	-6.09	-9.68	-5.65	-4.89	-7.10
16	1.32	9.85	-2.79	2.39	11.30	-1.50

MCS Index	CEESM SC LR	CEESM SC OAH	CEESM SC LHL	EESM SC LR	EESM SC OAH	EESM SC LHL
2	-21.10	-23.20	-20.19	-17.64	-19.93	-17.91
7	-19.72	-24.51	-20.36	-18.47	-22.54	-19.43
12	-7.34	-4.81	-10.25	-5.72	-2.64	-7.89
17	1.13	5.15	0.48	2.80	6.56	0.72

TABLE III: MSE values (in dB) of CEESM and EESM schemes for OFDM/ SC modes under various TGay environments

reason is that LHL is a reflection-rich environment. When a 2-by-2 antenna array is employed with wider half-power beam width (HPBW) in LHL environment, compared to a 4-by-4 antenna array in LR environment, some paths with strong power could have large delays, which makes the guard interval not sufficient to handle IBI for both OFDM and SC modes. In contrast to OFDM mode, the BER predicted using MMIB for SC mode does not match well with the LLS results for all three TGay channels when high order MCSs are employed, as shown in Fig. 5(b). The reason is that apart from the above-mentioned LHL environment issue, the SC mode is subject to the post-processing residual ISI at the RX with MMSE-FDE even when the path delays are within the guard interval length, which is not taken into account while computing the effective SNR in MMIB. Therefore, the residual ISI increases (or decreases) when the signal power increases (or decreases).

Fig. 5(c) demonstrates the BER/SNR validation comparison of PPESM for SC mode transmission in LR, OAH and LHL environments. It can be observed that the PPESM BER samples are closer to the AWGN curves when comparing with the MMIB results in Fig. 5(b), especially for LHL environment. This is owing to the fact that the PPESM is aware of the residual ISI while computing the effective SNR through post-processing SNR (c.f. (6)). However, some gap still exist between the predicted BER using PPESM and the BER from LLS for high order MCS, since the high order modulation schemes are more sensitive to the residual ISI, which in turn generates the distortion. Further note that this distortion is hard to remove unless employing a more advanced equalizer with a cost of higher complexity.

V. Final Remarks

In this paper, we have addressed the L2S level mapping for OFDM and SC modes in IEEE 802.11ay WLAN systems

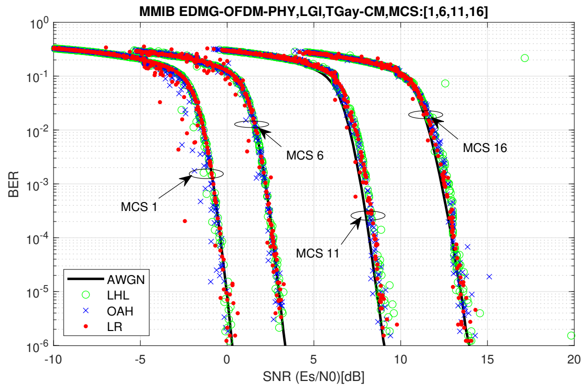

(a) MMIB OFDM mode

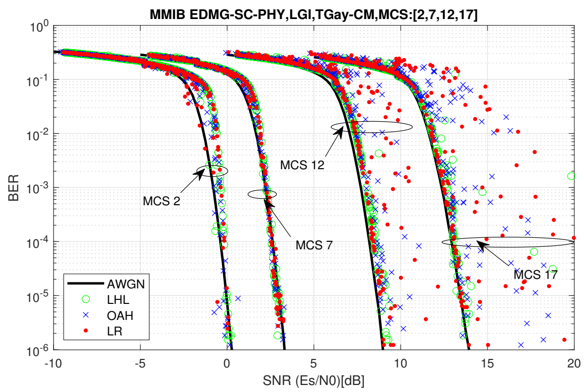

(b) MMIB SC mode

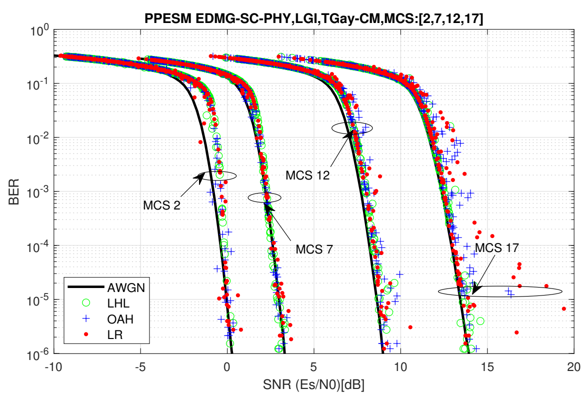

(c) PPESM SC mode

Fig. 5: MMIB and PPESM validation considering various MCSs (BPSK, QPSK, 16-QAM, 64-QAM all in $1/2$ code rate)

over the 60 GHz mmWave band using the Q-D channel model generated based on real measurements. We have studied the performance of the three existing ESM schemes (i.e., EESM, MMIB, PPESM) which were originally proposed for OFDMA and SC-FDMA systems and on sub-6 GHz bands. We have also designed the CEESM scheme by incorporating a metric to measure the severity of frequency-selective fading. To validate the feasibility of these schemes, we have conducted extensive simulations. Our experimental results confirm that EESM and CEESM achieve the highest accuracy but with the initial calibration cost. We compare the performance for three environments (LR, OAH and LHL), and confirm that

MCS Index	MMIB OFDM		
	LR	OAH	LHL
1	-24.34	-24.49	-30.34
6	-24.15	-25.27	-28.38
11	-6.60	-8.54	18.89 (-6.19)
16	-1.72	3.21	26.53 (1.02)

MCS Index	MMIB SC			PPESM SC		
	LR	OAH	LHL	LR	OAH	LHL
2	-18.79	-19.52	-18.76	-18.63	-19.94	-18.04
7	-20.20	-21.46	-19.78	-19.81	-21.32	-20.69
12	9.41	3.11	18.88	-1.02	-2.72	-5.82
17	24.48	21.41	16.25	21.25	10.00	1.81

TABLE IV: MSE values (in dB)[9] of MMIB for OFDM/ SC modes and PPESM for SC Mode in various TGay environments

the mapping parameters calibrated using one environment can be applied to other environments, so that the mapping metric is more MCS and mode dependent rather than environment dependent. We also confirm that MMIB and PPESM, having very low implementation cost, provide reasonable performance for OFDM mode and SC mode, respectively. With the initial effort completed for the single link systems, we are currently working to extend this research to evaluate MIMO systems.

REFERENCES

[1] *Wireless LAN MAC and PHY Specifications–Amendment: Enhanced Throughput for Operation in License-Exempt Bands Above 45 GHz*, IEEE Std. IEEE P802.11ay/D4.0, June 2019.

[2] *IEEE 802.16m Evaluation Methodology*, IEEE Std. IEEE 802.16m-08/004r5, 2009.

[3] T. L. Jensen, S. Kant, J. Wehinger, and B. H. Fleury, "Fast link adaptation for MIMO OFDM," *IEEE Trans. Veh. Technol.*, vol. 59, no. 8, pp. 3766–3778, Oct 2010.

[4] F. L. Aguilar, G. R. Cidre, and J. R. París, "Effective SNR mapping algorithms for link prediction model in 802.16e," in *Proc. ICUMTW 2009*, Oct 2009, pp. 1–6.

[5] H. Liu, L. Cai, H. Yang, and D. Li, "EESM based link error prediction for adaptive MIMO-OFDM system," in *Proc. IEEE VTC2007-Spring*, April 2007, pp. 559–563.

[6] F. Jiang, Y. Xue, B. Jiang, and S. Jin, "Average effective SNR mapping in LTE-A uplink," in *Proc. IEEE ICCC 2012*, Aug 2012, pp. 403–407.

[7] Samsung, "3GPP TSG-RAN WG1 meeting #43: Simulation methodology for EUTRA uplink: SC-FDMA and OFDMA," 3GPP, Tech. Rep. Work Item R1-051352, Nov. 2005.

[8] Motorola, "3GPP TSG-RAN WG1 meeting #43: Simulation methodology for EUTRA UL: IFDMA and DFT-Spread-OFDMA," 3GPP, Tech. Rep. R1-051335, Nov. 2005.

[9] A. Bodi, J. Zhang, J. Wang, and C. Gentile, "Physical-layer analysis of IEEE 802.11ay based on a fading channel model from mobile measurements," in *Proc. IEEE ICC 2019*, May 2019, pp. 1–7.

[10] C. Lai and et al., "Methodology for multipath-component tracking in millimeter-wave channel modeling," *IEEE Trans. Antennas Propag.*, vol. 67, no. 3, pp. 1826–1836, March 2019.

[11] K. Brueninghaus and et al., "Link performance models for system level simulations of broadband radio access systems," in *Proc. IEEE PIMRC 2005*, vol. 4, Sep. 2005, pp. 2306–2311 Vol. 4.

[12] S. Nanda and K. M. Rege, "Frame error rates for convolutional codes on fading channels and the concept of effective Eb/N0," *IEEE Trans. Veh. Technol.*, vol. 47, no. 4, pp. 1245–1250, Nov 1998.

[13] *IEEE P802.11 Wireless LANs TGay Evaluation Methodology*, IEEE Std. IEEE 802.11-09/0296r16, 2016.

[14] J. Zhang, L. Yang, and L. Hanzo, "Frequency-domain turbo equalisation in coded SC-FDMA systems: EXIT chart analysis and performance," in *Proc. IEEE VTC-Fall 2012*, Sep. 2012, pp. 1–5.

[15] *Channel Models for IEEE 802.11ay*, IEEE Std. IEEE 802.11-15/1150r9, 2016.